THE JOURNAL OF BIOLOGICAL CHEMISTRY VOL. 284, NO. 28, pp. 18994–19005, July 10, 2009
Printed in the U.S.A.

Xenopus SMOC-1 Inhibits Bone Morphogenetic Protein Signaling Downstream of Receptor Binding and Is Essential for Postgastrulation Development in *Xenopus*[S]

Received for publication, October 7, 2008, and in revised form, February 26, 2009 Published, JBC Papers in Press, May 4, 2009, DOI 10.1074/jbc.M807759200

J. Terrig Thomas[‡1], **Paola Canelos**[‡], **Frank P. Luyten**[§], **and Malcolm Moos, Jr.**[‡2]

From the [‡]*Division of Cellular and Gene Therapies, Center for Biologics Evaluation and Research, United States Food and Drug Administration, Bethesda, Maryland 20892 and the* [§]*Laboratory for Skeletal Development and Joint Disorders, Division of Rheumatology, Department of Musculoskeletal Sciences, Katholieke Universiteit Leuven, 3000 Leuven, Belgium*

The bone morphogenetic protein (BMP) family of signaling molecules and their antagonists are involved in patterning of the body axis and numerous aspects of organogenesis. Classical biochemical purification and protein sequencing of highly purified fractions containing potent bone forming activity from bovine cartilage identified several BMPs together with a number of other proteins. One such protein was SMOC-2 (secreted modular calcium-binding protein-2), classified as belonging to the BM-40 family of modular extracellular proteins. Data regarding the biological function of SMOC-2 and closely related SMOC-1 remain limited, and their expression or function during embryological development is unknown. We therefore isolated the *Xenopus* ortholog of human SMOC-1 (XSMOC-1) and explored its function in *Xenopus* embryos. In gain-of-function assays, XSMOC-1 acted similarly to a BMP antagonist. However, in contrast to known extracellular ligand-binding BMP antagonists, such as noggin, SMOC antagonizes BMP activity in the presence of a constitutively active BMP receptor, indicating a mechanism of action downstream of the receptor. We provide several lines of evidence to suggest that SMOC acts downstream of the BMP receptor via MAPK-mediated phosphorylation of the Smad linker region. Loss-of-function studies, using antisense morpholino oligonucleotides, revealed XSMOC-1 to be essential for postgastrulation development. The catastrophic developmental failure observed following XSMOC knockdown resembles that observed following simultaneous depletion of three ligand-binding BMP antagonists described in prior studies. These findings provide a direct link between the extracellular matrix-associated protein SMOC and a signaling pathway of general importance in anatomic patterning and cell or tissue fate specification.

Patterning of the body axis, axial and appendicular skeleton, and various other structures requires many interacting signals expressed in complex spatial and temporal patterns. Among these signals are the bone morphogenetic proteins (BMPs)[3] and their antagonists (for a review, see Ref. 1). Several proteins in the BMP subgroup of the transforming growth factor superfamily were identified by classical biochemical purification and protein sequencing of fractions containing potent bone forming activity from bovine cartilage (2). These fractions also contained proteins unrelated to the BMPs structurally, such as the Wnt antagonist Frzb (3). Another protein, which could not be dissociated from osteoinductive activity following extensive purification, was identified as SMOC-2 (secreted modular calcium-binding protein-2).[4] SMOC-2 and the closely related SMOC-1 have been classified as belonging to the BM-40 family of modular extracellular proteins (4, 5), because they contain a follistatin-like domain and a C-terminal extracellular calcium-binding domain (4, 5). They also contain two thyroglobulin-like domains and a novel domain without known homologs. The extracellular calcium-binding domain has been shown to bind calcium (5), but data regarding the biological function of SMOC1/2 remain limited. Furthermore, there are currently no published data on SMOC-1/2 function during embryological development. Both proteins are expressed in a wide variety of adult mouse tissues and are secreted by established cell lines of epithelial and mesenchymal origin. Immunofluorescence analyses have shown SMOC-1/2 to be associated with basement membrane structures (4, 5), and human vascular endothelial cells infected with adenovirus expressing SMOC-2 show SMOC-2 to be localized predominantly to the cell periphery (6). These data are consistent with a putative role of SMOC-2 as a regulator of extracellular matrix interactions and/or growth factor signaling. The related BM-40 family member SPARC (secreted protein acidic and rich in cysteine) binds to platelet-derived growth factor (7) and vascular endothelial growth factor (8) and indirectly influences the effects of basic fibroblast growth factor (9) and transforming growth factor β (10). In cell culture, SMOC-2 has been shown to potentiate cellular responses to basic fibroblast growth factor and vascular endothelial growth factor (6) and the mitogenic effects of epidermal growth factor and platelet-derived growth factor (11).

[S] The on-line version of this article (available at http://www.jbc.org) contains supplemental Figs. S1 and S2.

[1] To whom correspondence may be addressed. E-mail: john.thomas@fda.hhs.gov.

[2] To whom correspondence may be addressed. E-mail: malcolm.moos@fda.hhs.gov.

[3] The abbreviations used are: BMP, bone morphogenetic protein; SMOC, secreted modular calcium binding protein; MAPK, mitogen-activated protein kinase; RT, reverse transcription; MES, 4-morpholineethanesulfonic acid; ERK, extracellular signal-regulated kinase; dp-ERK, diphospho-ERK; Tricine, *N*-[2-hydroxy-1,1-bis(hydroxymethyl)ethyl]glycine; caBMPR1B, constitutively active chicken BMP receptor 1B; LM-Smad1, linker mutant Smad1; MEK, mitogen-activated protein kinase/extracellular signal-regulated kinase kinase; GFP, green fluorescent protein; MO, morpholino; XSMOC-1, *Xenopus* SMOC-1; XSox2, *Xenopus* Sox2; XNot, *Xenopus* Not; XMyf5, *Xenopus* Myf5; XVent-1, *Xenopus* Vent-1.

[4] M. Moos and F. P. Luyten, unpublished observations.

The biochemical studies described above, together with the co-purification of SMOC with BMPs (2),[4] suggested the possibility of a functional role during embryonic development. *Xenopus* provides a powerful system in which to examine gene function by both gain and loss of function. We therefore isolated the *Xenopus* ortholog of human SMOC-1 (XSMOC-1) and explored its function in *Xenopus* embryos. In gain-of-function assays, XSMOC-1 acted as a BMP antagonist, and loss-of-function studies revealed XSMOC-1 to be essential for postgastrulation development. In contrast to BMP antagonists described to date, several lines of evidence suggest that XSMOC-1 acts intracellularly, via the mitogen-activated protein kinase (MAPK) signaling pathway, rather than by extracellular binding to the ligands themselves.

EXPERIMENTAL PROCEDURES

Isolation of Xenopus SMOC-1—Initial cDNA sequences encoding *Xenopus* SMOC were obtained following 5′- and 3′-SMART™-RACE (Clontech) amplification using mRNA from stage 59 limbs and degenerate primers designed to sequences conserved between human SMOC1/2 located at the boundary of the follistatin-like and thyroglobulin-like domain 1 (5′-CCACACAYYTGGRYRYRTCTTTGCA-3′) and the extracellular calcium-binding domain (5′-TGGARGCVCTCWCCACHGACATGGT-3′). Full-length *Xenopus* SMOC-1 (accession number EU287947) was obtained by reverse transcription (RT)-PCR using stage 59 limb cDNA and the primers 5′-CCTTCATACAAGTCTCACGCCTGA-3′ and 5′-CTTCTTCTGGCCGGCTCTCCTA-3′. PCR products were cloned into pCR®4-TOPO (Invitrogen) and confirmed by sequencing. XSMOC-1 was subsequently subcloned into pCS2 and pcDNA3.

Plasmids and Probes—Zebrafish SMOC-2, obtained from the Zebrafish International Resource Center (clone ID CB488) as full-length expressed sequence tag in pSPORT1, was subcloned into pCS2 (provided by David Turner). BMP2, activin, and linker mutant Smad1 (LM-Smad1) were kind gifts from Gerald Thomsen, Sergei Sokol, and Joan Massagué, respectively. Noggin was isolated from stage 10.5 *Xenopus* cDNA by RT-PCR and confirmed by sequencing in both directions. Constitutively active chicken BMPR1B was kindly provided by Lee Niswander in the avian retroviral expression vector RCAS BP(A), from which the open reading frame was amplified by PCR using the primers 5′-GTTTTCTGGACAAGATGCCCTT-3′ and 5′-CTCCATCAGAGCTTAATGTCCT-3′. The product was sequenced and subcloned into pCS2. XSox2 (image clone 3398743) and XNot (image clone 8318484) were in pCMVSport6 and pExpress, respectively. XMyf5 was isolated by RT-PCR using mRNA from stage 11 *Xenopus* embryos and was subcloned into PCR-Script™ (Stratagene). *Xenopus* SMOC-1 antisense morpholino oligonucleotides were as follows: XSMOC-1 MO (5′-GTCATGTTGCCTCTTCTTATACAGG-3′), XSMOC-1 MO 5-base mismatch control (5′-GTgATcTTGCgTCTTgTTATAgAGG-3′), and XSMOC-1 MO2 (5′-CAATCAGGCGTGAGACTTGTATGAA-3′). Each was tagged with fluorescein and purchased from Gene Tools.

Embryo Manipulations—Frogs and their embryos were maintained and manipulated using standard methods (12, 13). All embryos were staged according to Nieuwkoop and Faber (14) and Keller (15). mRNA injection experiments were performed by standard procedures, as described previously (16). Dorsal and ventral blastomeres were identified by size and pigment variations (14). Animal cap explants were cultured in 0.7× Marc's modified Ringer's solution (13) containing 1 mg/ml bovine serum albumin and 50 μg/ml gentamicin. mRNAs were injected into both blastomeres at the two-cell stage or dorsal blastomeres at the four-cell stage. For conjugated animal cap assays, animal caps were removed from stage 9 embryos, conjugated immediately, and cultured in 0.7× Marc's modified Ringer's solution, 1 mg/ml bovine serum albumin, 50 μg/ml gentamicin until noninjected siblings reached stage 17.

Perturbations of axial patterning were quantified by dorsoanterior index (17). Dark field images of embryos were photographed with low angle oblique illumination and a Zeiss Stemi-6 dissecting microscope.

Immunoblotting—XSMOC-1 (300 pg) was injected equatorially into each blastomere of *Xenopus* embryos at the four-cell stage, and animal caps, isolated at stage 9, were incubated in 0.7× Marc's modified Ringer's solution, 1 mg/ml bovine serum albumin. 50 μg/ml gentamicin until sibling embryos reached stage 17. Animal caps were extracted on ice in 20 mM Tris, pH 7.5, 5 mM EDTA, 2 mM EGTA, 30 mM sodium fluoride, 40 mM β-glycerophosphate, 20 mM sodium pyrophosphate, 1 mM sodium orthovanadate, 1 mM phenylmethylsulfonyl fluoride, 3 mM benzamidine, 5 μM pepstatin A, 10 μM leupeptin, and 0.5% Nonidet P-40 in a volume of 10 μl/cap. Supernatants (10 μg/lane) were analyzed by SDS-PAGE using Novex 10% NuPAGE gels and the MES buffer system. Immunoblot analysis was performed using the mini-PROTEAN II system (Bio-Rad) and Immobilon™-P polyvinylidene difluoride membranes (Millipore). The diphospho form of extracellular signal-regulated kinase (dp-ERK) was detected using the rabbit phospho-p44/42 MAPK primary antibody (Cell Signaling), goat anti-rabbit horseradish peroxidase-conjugated secondary antibody (Pierce), and SuperSignal® West Femto Maximum Sensitivity Substrate (Pierce).

RT-PCR—Separate pools of embryos or explants from at least two different fertilizations were prepared and analyzed for each condition reported. Total RNA was prepared with Trizol™ Invitrogen and treated with DNA-free™ DNase removal reagent (Ambion). RT was done using Taqman® RT reagents (Applied Biosystems) as described by the manufacturer, using 1 μg of total RNA/reaction; 2% of the cDNA obtained was used in each PCR. Amplification was performed in 10-μl reactions containing 40 mM Tricine-KOH, pH 8.7, 15 mM KOAc, 3.5 mM $Mg(OAc)_2$, 0.375% bovine albumin, 2.5% Ficoll 400, 5 mM cresol red, 200 μM dNTPs, 0.5 μM each primer, and 0.2 units of Advantage® 2 polymerase (Clontech). Each cycle comprised 94 °C for 0 s, 55 °C for 0 s, and 72 °C for 40 s; a 1-min denaturation at 94 °C preceded cycling, and a 2-min extension at 72 °C was included after the final cycle. An Idaho Technologies air thermal cycler was used in all experiments, allowing momentary (setting of "0 s") dwell times at the annealing and denaturation temperatures to increase amplification specificity. Optimal cycle numbers and annealing temperatures were

determined for each primer set. PCR products were separated on 2% agarose gels in TAE buffer, stained with SYBR Green 1™ (Molecular Probes, Inc., Eugene, OR), and scanned using an Amersham Biosciences Fluorimager. PCR analysis was performed at least twice for each cDNA to confirm that the amplifications were reproducible. The *Xenopus* primers for histone H4, Brachyury, cardiac actin, engrailed, keratin, Krox-20, N-CAM, N-tubulin, and Otx2 are given in Xenbase (available on the World Wide Web); those for Myf-5, Pax6, and XAG-1 are given by the De Robertis laboratory (available on the World Wide Web); those for XVent-1 are from Ref. 48; and those for NRP-1 are 5′-GAGTCGCCAGAGACCGAATGGA-3′ and 5′-CATGGCATCATCCACCTTCCCAA-3′.

Hybridization in Situ— cRNA probes were produced using MEGAscript T3, T7, or SP6 *in vitro* transcription kits (Ambion), incorporating digoxigenin. For whole mount hybridization *in situ* on *Xenopus* embryos, procedures outlined by Harland were followed (18), with modifications as described (16). For colorimetric detection, signals were developed using alkaline phosphatase-conjugated antibodies to digoxigenin and BM-Purple (Roche Applied Science). Overstained embryos were embedded in JB-4 resin (Polysciences, Warrington, PA) after abbreviated infiltration (3 × 10 min) and sectioned at 20 μm with a Leica RM2265 rotary microtome.

Histology—Paraffin-embedded embryos were sectioned at 7 μm and stained using a modification the Feulgen, light green, orange G method (19). Briefly, deparaffinized sections were incubated overnight at room temperature in fresh Feulgen stain, rinsed, incubated for 5 min in light green (0.2% in 95% ethanol), rinsed, and incubated for 30 min in orange G (0.2% in 0.2% phosphotungstic acid).

Embryos embedded in JB-4 resin, according to the manufacturer's instructions, were sectioned at 3 μm. To accentuate the cement gland and clearly differentiate yolk platelets from other tissues, a modified Van Gieson stain was used. Sections were stained for 1 h in 1% Celestine Blue, 5% ferric ammonium sulfate; washed in water; stained in 3× Weigert's hematoxylin (3% in 95% ethanol) for 30 s; and rinsed sequentially with water, 0.37% HCl in 70% ethanol, and 0.07% ammonia in water. The acid alcohol wash was for 2–5 dips, sufficient to remove background Celestine Blue stain; the ammonia water staining was similar, but the appearance of a light blue background was used as the stopping point. After a 20-min water wash, the embryos were stained with Van Gieson's solution (20 ml of 1% acid fuchsin in water plus 25 ml saturated picric acid) until adequate color balance was achieved (2–5 min). Picric acid was from Fluka; all other reagents were from Sigma.

Cell Culture—Mouse 3T3 fibroblasts (1×10^6) were transiently transfected with 3 μg of pcDNA3 or pcDNA3-XSMOC-1 using Nucleofector kit R (Amaxa Biosystems). Following transfection, cells were cultured in Dulbecco's modified Eagle's medium, 10% fetal calf serum for 18 h and then incubated in serum-free Dulbecco's modified Eagle's medium for 30 min before the addition of recombinant human BMP2 (Cell Signaling) for 1 h. Medium was removed, and cell lysates were extracted in 6 M urea, 25 mM Tris, 2% SDS containing Halt™ protease and phosphatase inhibitors (Thermo Scientific). BMP2 activity was determined by SDS-PAGE followed by immunoblot analysis of phospho-Smad1, -5, and -8 (the phosphorylation site is conserved among each paralog) and Smad1 (Cell Signaling) using an Odyssey imager and IRDye®800-labeled secondary antibodies (LI-COR Biosciences).

RESULTS

Isolation and Characterization of Xenopus SMOC—Although mammals have two forms of SMOC, extensive attempts to isolate more than one form from *Xenopus* were unsuccessful, and searches of *Xenopus* (*laevis* and *tropicalis*) expressed sequence tag data bases and the Joint Genome Institute *Xenopus tropicalis* genomic data base (version 4.1) revealed only a single form. The *Xenopus* SMOC open reading frame is 74 and 50% identical to human SMOC-1 and SMOC-2, respectively. Therefore, the gene product is most likely the *Xenopus* ortholog of human SMOC-1. XSMOC-1 is composed of 463 amino acids, compared with 434 in human SMOC-1. The difference is due largely to an additional 19 amino acids at the C-terminal end and an additional 9 amino acids within a domain that lacks homology to other proteins (termed the nonhomologous domain). The domain structure of XSMOC-1 and mammalian SMOC1/2 is conserved (see Fig. S1). XSMOC-1 has a 25-amino acid leader sequence, followed by a predicted signal peptidase cleavage site between amino acids 25 and 26 (CFG-R). The identities between human SMOC-1 and XSMOC-1 within the conserved domains of the mature protein are as follows: follistatin-like domain, 72%; thyroglobulin-like domain 1, 93%; nonhomologous domain, 42%; thyroglobulin-like domain 2, 79%; calcium-binding domain, 88%.

XSMOC-1 first became detectable by RT-PCR at stage 12.5, corresponding to late gastrulation/early neurulation, and remained at consistent levels throughout neurula and tail bud stages (Fig. 1*A*). Hybridization *in situ* in whole embryos showed XSMOC-1 to be expressed initially at stage 12.5 at the anterior of the embryo with a dorso-ventral distribution (Fig. 1*B*). At stage 14, XSMOC-1 was localized within the anterior-ventral region and also lateral to the developing neural plate (Fig. 1*C*). This staining pattern continued throughout neurulation (Fig. 1, *C–E*). At later stages (stages 20–25), XSMOC-1 was localized dorsal to the cement gland, the ventral region of the developing eye Fig. 1*H*), and the developing pronephros (Fig. 1, *F–J*). Expression was also observed in the mesencephalon and rhombencephalon (Fig. 1, *I* and *J*) with prolonged color development. By stage 30, XSMOC-1 was also observed in the pharyngeal arches (not shown). Transverse sections of overstained embryos at stage 25 confirmed the ventral eye expression domain (Fig. 1*K*) and revealed XSMOC-1 to be localized to the lateral regions of the midbrain (not shown) and hindbrain (Fig. 1*L*). In the trunk, expression was observed throughout the pronephros and in subepithelial neural crest cells migrating laterally to the somites (Fig. 1*M*).

Gain of Function of XSMOC-1 Produces a Phenotype and Molecular Marker Pattern Consistent with Action as a BMP Antagonist—Bilateral injection of mRNA (300 pg) encoding XSMOC-1 (Figs. 2 and 3) or zebrafish SMOC-2 (not shown) at the two-cell stage produced exaggerated dorsal/anterior structures, most prominently enlarged heads and cement

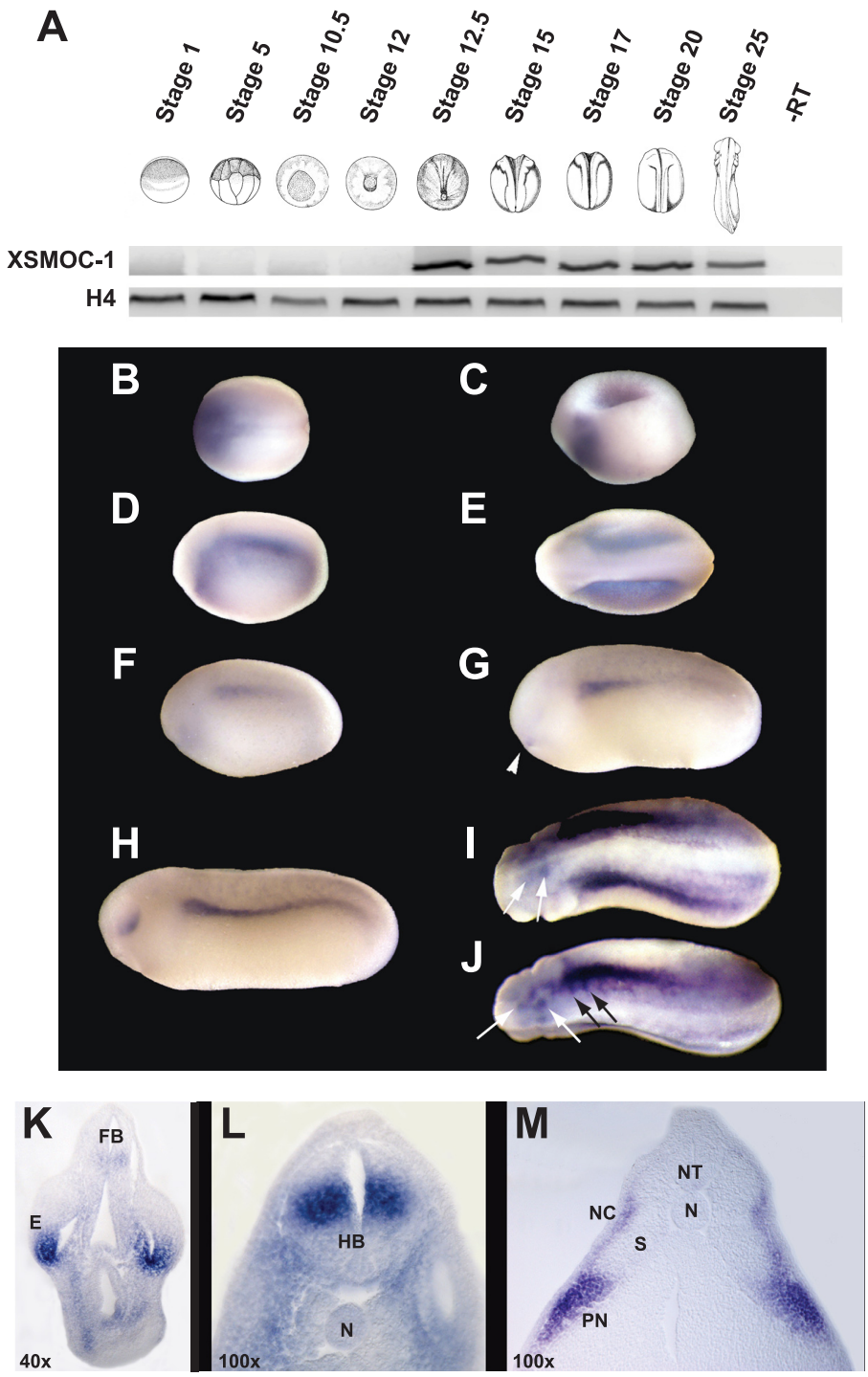

FIGURE 1. **Expression of XSMOC-1 during embryogenesis.** *A*, RT-PCR analysis of XSMOC-1 expression at different stages of development. XSMOC-1 was not detectable until after stage 12. Histone H4 is shown as positive control, and *−RT* indicates RT-PCR without reverse transcriptase as negative control. *B–I*, whole mount hybridization *in situ* analysis of XSMOC-1 (anterior to the *left*). *B*, ventral view of a stage 12.5 embryo showing anterior staining. *C*, ventro-lateral view of a stage 15 embryo showing anterior and lateral staining. Shown are lateral (*D*) and dorsal (*E*) view of a stage 17 embryo showing staining lateral to the neural plate. *F–H*, lateral views showing XSMOC-1 expression throughout the developing pronephros at stage 20 (*F*), stage 22 (*G*), and stage 24 (*H*). At stage 22 (*G*), additional expression was observed dorsal to the cement gland (*arrowhead*), and from stage 25 (*H*) onward, XSMOC-1 was expressed in the ventral region of the developing eye. *I* and *J*, dorsal views of *H*, following prolonged color development, showed expression in the mesencephalon, rhombencephalon (*white arrows*), and migrating neural crest (*black arrows*). *K–M*, transverse sections through the embryos shown in *I* and *J* in the region of the forebrain (*K*), hindbrain (*L*), and anterior trunk (*M*). Staining was prominent in the ventral aspect of the developing eye (*K*) and in the lateral regions of the hindbrain (*L*). Within the trunk (*M*), staining was observed in the pronephros and in subepithelial migrating neural crest cells. *E*, eye; *FB*, forebrain; *HB*, hindbrain; *N*, notochord; *NC*, neural crest; *NT*, neural tube; *S*, somite.

glands. The phenotype was apparent at stage 17 (Fig. 2*B*). Whole mount hybridization *in situ* analysis of Sox2 expression demonstrated that relative to controls (Fig. 2*C*), the neural plate was expanded in the dorsalized embryos (Fig. 2*D*). Transverse sections taken through the anterior region of overstained embryos showed that, unlike controls (Fig. 2*E*), Sox2 expression occupied the majority of the tissue dorsal to the archenteron roof in XSMOC-1-overexpressing embryos (Fig. 2*F*). By stage 26, the dorsalization was more apparent (Fig. 3*B*), and histological analysis of sagittal sections revealed grossly hypertrophied columnar epithelium in the cement gland (Fig. 3*D*). Transverse sections through stage 33 XSMOC-1-overexpressing embryos showed enlargement of the neural tube and disorganized somites (Fig. 3*F*). Animal cap explants from embryos injected with XSMOC-1 mRNA expressed anterior neuroectodermal (Otx2 and XAG-1) and panneural (NCAM and NRP-1) markers but not the posterior neural marker Krox-20 (Fig. 4*A*). In addition, the epithelial marker keratin was down-regulated (Fig. 4*A*), supporting conversion from epithelial to neural cell fate. The biological effects of XSMOC-1 overexpression in these assays were consistent with that of a BMP antagonist (20, 21).

To examine whether XSMOC-1 action is cell-autonomous or is effective away from its point of origin, we assayed conjugated animal caps by whole mount hybridization *in situ*. Animal caps from wild-type embryos injected with control or XSMOC-1 mRNAs were conjugated to noninjected albino animal caps and analyzed by hybridization *in situ* for the anterior neuroectodermal marker Otx2 when sibling embryos reached stage 17. Otx2 was not detectable in the controls (Fig. 4*B*) but was readily detectable in the albino noninjected caps conjugated to XSMOC-1-expressing wild-type

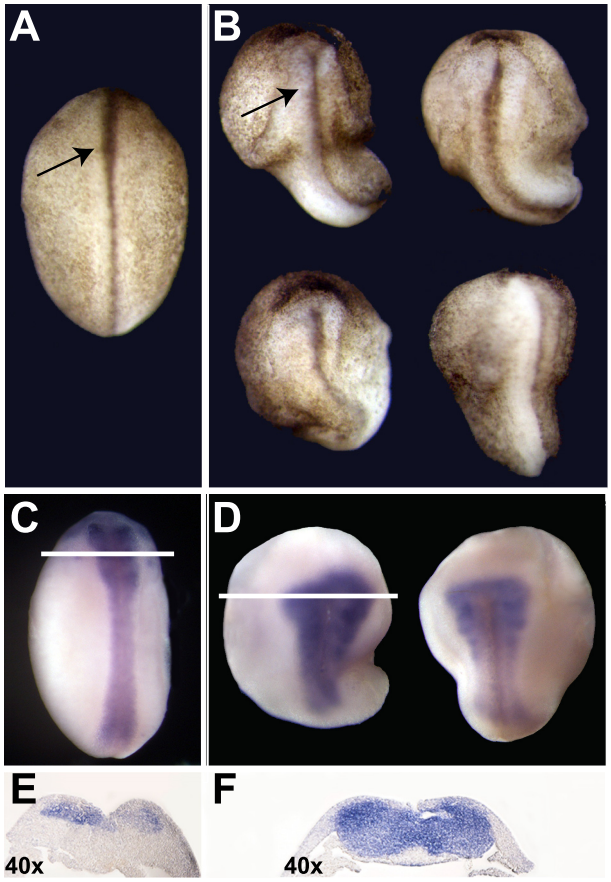

FIGURE 2. ***Xenopus* embryos overexpressing XSMOC-1 exhibit a dorsalized phenotype.** *A–D*, dorsal views of stage 17 embryos injected bilaterally at the two-cell stage with 300 pg of GFP (*A* and *C*) or XSMOC-1 (*B* and *D*) mRNAs. XSMOC-1-injected embryos have exaggerated anterior and diminished posterior structures (*B*) with laterally expanded expression of the neural plate marker Sox2 (*D*). The *arrows* indicate the position of the neural tube. *E* and *F*, transverse sections taken through the anterior regions of overstained embryos *C* and *D* (*white bars*) show Sox2 expression throughout the dorsal tissues in XSMOC-1-injected embryos (*F*). The phenotypes shown for XSMOC-1 overexpression are typical for this stage and were observed in 95% of the embryos in three separate experiments ($n = 96$).

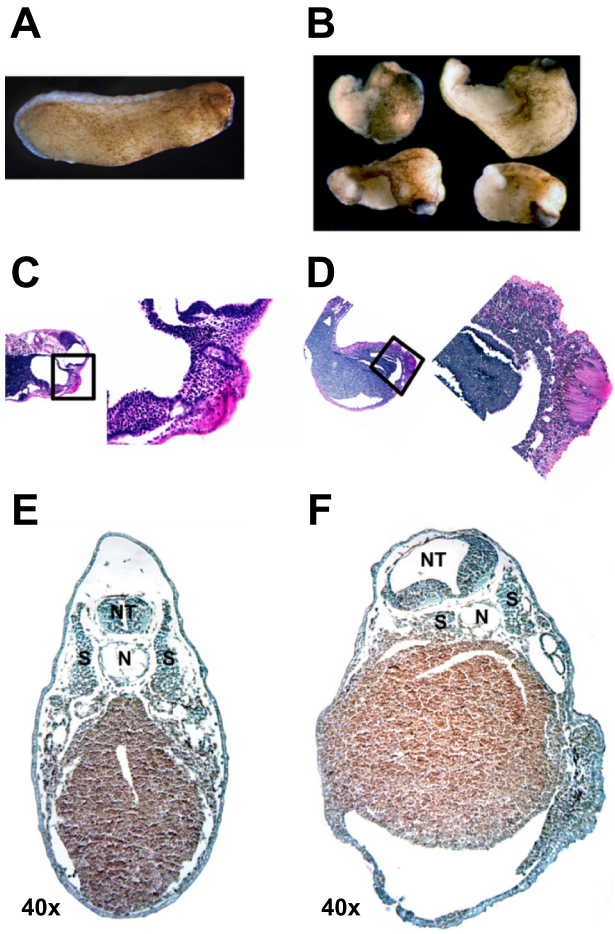

FIGURE 3. **Dorsalization is pronounced in tadpoles overexpressing XSMOC-1.** *A–F*, stage 26 *Xenopus* embryos injected bilaterally at the two-cell stage with 300 pg of GFP (*A*, *C*, and *E*) or XSMOC-1 mRNAs (*B*, *D*, and *F*). XSMOC-1-injected embryos were dorsalized, with exaggerated dorsal/anterior structures, particularly cement glands. The XSMOC-1 overexpression phenotypes shown in *B* were typical for this stage and were observed in 95% of the embryos in five independent experiments ($n = 218$). *C* and *D*, histological 3-mm plastic sections (modified Von Gieson stain) showing hypertrophic cement gland cells in XSMOC-1-overexpressing embryos (*D*). *E* and *F*, 7-mm paraffin sections (Feulgen, light green, orange G method) showing enlargement of the neural tube and disorganized somites in XSMOC-1-overexpressing embryos (*F*).

caps (Fig. 4*C*), indicating that XSMOC-1 can act at a distance from its cellular origin.

Loss of Function of XSMOC-1 Arrests Development at Neurulation—Injection of *Xenopus* embryos with morpholino antisense oligonucleotides has been used widely and effectively to study the effects of blocking the synthesis of selected proteins (22). An antisense morpholino to XSMOC-1 (XSMOC-1 MO) located at positions −20 to +5 was designed to examine the effect of down-regulation of XSMOC-1 during early *Xenopus* development. Initial studies were conducted on embryos injected unilaterally with 6 ng of XSMOC MO at the two-cell stage (Fig. 5). At stage 17, mild abnormalities were observed in the developing neural axis (Fig. 5*B*). By stage 32, compared with controls (Fig. 5*C*), anterior defects (mild ventralization) were apparent (Fig. 5, *D* and *E*), and eye and other anterior structures were absent or severely dysmorphic on the injected side; corresponding structures on the noninjected side were also affected but less severely (Fig. 5, *D* and *E*). At stage 38, these differences were more obvious (Fig. 5*G*). Whole mount hybridization *in situ* studies of stage 32 embryos for Otx2 (Fig. 5, *H* and *I*) and Tbx2 (Fig. 5, *J* and *K*) revealed aberrant expression of these markers in the eye field on the XSMOC-1 MO-injected side (Fig. 5, *I* and *K*, *right*). Otx2 expression was diminished in the developing eye field on the noninjected side and was completely absent on the MO-injected side (Fig. 5*I*). Expression of Tbx2 on the noninjected side was similar to that of controls (Fig. 5, *J* and *K*, *left*), but expression in the eye field was diminished (Fig. 5*K*, *left*). On the MO-injected side, Tbx2 expression was absent from the eye region and branchial arches but was present in the cranial ganglia, otic vesicle, and frontonasal process (Fig. 5*K*, *right*).

Bilateral injections of 6 ng of XSMOC MO at the two-cell stage resulted in complete developmental arrest at the end of gastrulation (Fig. 6). Development appeared normal until late gastrulation (Fig. 6, *D* and *E*), and RT-PCR analyses revealed normal expression of the markers Brachyury, Goosecoid, and Myf-5 at stage 10.5 (Fig. 6*G*) and of cardiac actin, Otx2, and XAG at stage 12 (Fig. 6*H*). Developmental arrest immediately

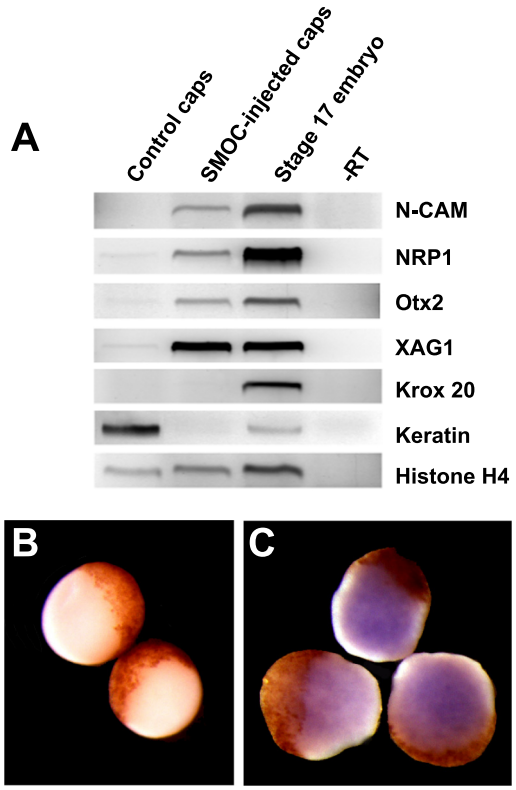

FIGURE 4. **XSMOC-1 induces neural markers in animal cap explants and acts non-cell-autonomously.** *A*, RT-PCR analysis of animal caps obtained from embryos injected bilaterally with 300 pg of GFP (control) or XSMOC-1 at the two-cell stage. Animal caps were removed from stage 8 embryos and cultured until noninjected siblings reached stage 17. XSMOC-1 induced the neural markers N-CAM, NRP1, Otx2, and XAG1 and suppressed the expression of the epidermal marker, keratin. mRNA extracted from whole embryos (*lane 3*) was used as a positive control for the RT-PCRs, and reactions from which reverse transcriptase was omitted (−*RT*; *lane 4*) were the negative controls. *B* and *C*, whole mount hybridization *in situ* of Otx2 in albino animal caps conjugated to wild-type caps. Wild-type embryos were injected bilaterally with 300 pg of GFP (*B*) or XSMOC1 (*C*). Animal caps were removed at stage 8 and conjugated to caps removed from stage 8 noninjected albino embryos. The conjugates were cultured until sibling embryos reached stage 17. Otx2 staining was not observed in the GFP control cap conjugates (*B*) but was present in the noninjected albino caps conjugated to XSMOC1-injected wild-type caps (*C*).

prior to neurulation appeared to be very abrupt and nearly total (Fig. 6*F*); the postgastrulation markers En-2, Pax6, and N-tubulin were expressed only weakly (Fig. 6*I*). Hybridization *in situ* analyses at stage 11–11.5 demonstrated some disturbance of the normal expression patterns of the organizer and presumptive notochord marker XNot and the myogenic marker Myf5 in XSMOC-1 MO-injected embryos (Fig. 7, *A–D*). At stage 12.5, XNot expression in the presumptive notochord of XSMOC-1 MO-injected embryos was abnormal, and the neural plate marker XSox2 was disturbed severely (Fig. 7, *E–H*). At stage 15, convergent extension associated with neurulation failed to occur in XSMOC-1 MO-injected embryos, and the XSox2 expression pattern was disrupted further (Fig. 7, *I* and *J*). Histological analysis of these embryos revealed the absence of the archenteron and any recognizable dorsal structures (Fig. 7*L*). These findings suggest that the effects of XSMOC-1 loss of function are specific to one or more processes occurring near the end of gastrulation and are not due to disruption of a more global process necessary for cell viability.

The specificity of the XSMOC-1 morpholino effect on *Xenopus* embryos was confirmed as follows. Co-injection of XSMOC-1 MO (12 ng) with zebrafish SMOC-2 mRNA (600 pg), which cannot hybridize to XSMOC-1 MO, produced partial to full rescue of bilaterally injected embryos (see Fig. S2). Injection of a second nonoverlapping XSMOC-1 antisense MO located at positions −39 to −63 (XSMOC-1 MO2) produced the same phenotype as XSMOC-1 MO (65% of embryos arrested prior to neurulation in three separate experiments; $n = 96$) in bilaterally injected embryos, at a dose of 30 ng/blastomere at the two-cell stage (not shown).

XSMOC-1 Blocks the Effects of BMP2 but Not Activin and Acts Downstream of the BMPR1B Receptor—Since overexpression of XSMOC-1 in *Xenopus* embryos produced a phenotype similar to that observed for BMP antagonists, we analyzed the effect of XSMOC-1 on BMP2 and activin activity. Both are members of the transforming growth factor β superfamily but signal via different serine-threonine kinase receptors. Overexpression of BMP2 in *Xenopus* embryos produced a strongly ventralized phenotype (23) (Fig. 8*A*) that could be rescued partially or completely by co-expression of XSMOC-1 (Fig. 8*A*). RT-PCR analysis demonstrated that BMP2-mediated induction of the ventral marker XVent-1 was blocked completely by co-expression of XSMOC-1 in animal cap explants (Fig. 8*B*). In contrast, induction of Brachyury by activin was not inhibited by XSMOC-1 (Fig. 8*C*). Inhibition of BMP2 activity by XSMOC-1 was also demonstrated in mammalian cell culture (Fig. 8*D*). Mouse 3T3 fibroblasts were chosen, since they have been shown previously to respond to exogenous BMP2/4/7 (24). Cells were transiently transfected with pcDNA3 or pcDNA3-XSMOC-1 and incubated in the presence or absence of recombinant human BMP2 at 50 or 100 ng/ml for 1 h. Analysis of cell lysates demonstrated that induction of phospho-Smad 1, 5, or 8 was inhibited by XSMOC-1 at both concentrations of BMP2 (Fig. 8*D*).

To investigate whether XSMOC-1 acts by direct binding to ligand, we studied its effect in the presence of the constitutively active chicken BMP receptor 1B (caBMPR1B). Overexpression of caBMPR1B has been shown to promote signaling of the BMP2/4/7 family in the absence of bound ligand (25), and, consistent with this expectation, animal cap explants from *Xenopus* embryos injected with caBMPR1B mRNA expressed the ventral marker XVent-1 (Fig. 8*E*). As expected, the BMP antagonist noggin, which acts extracellularly by direct ligand binding, did not reverse this effect (Fig. 8*E*). However, expression of XVent-1 in caps from embryos injected with both XSMOC-1 and caBMPR1B mRNA was expressed only weakly (Fig. 8*E*), indicating that XSMOC-1 does not inhibit BMP signaling via direct binding to BMPs. It also suggests that XSMOC-1 acts downstream of the BMP receptor.

BMP receptors signal through C-terminal phosphorylation of Smad (for a review, see Ref. 26). This can be inhibited by activation of the MAPK/ERK pathway, which results in Smad phosphorylation within the linker region, effectively blocking C-terminal phosphorylation (27–29). To evaluate the possibility that XSMOC-1 acts via this mechanism, we studied the effect of XSMOC-1 in the presence of LM-Smad1. LM-Smad1 has four serine-to-alanine substitutions at conserved P*X*SP

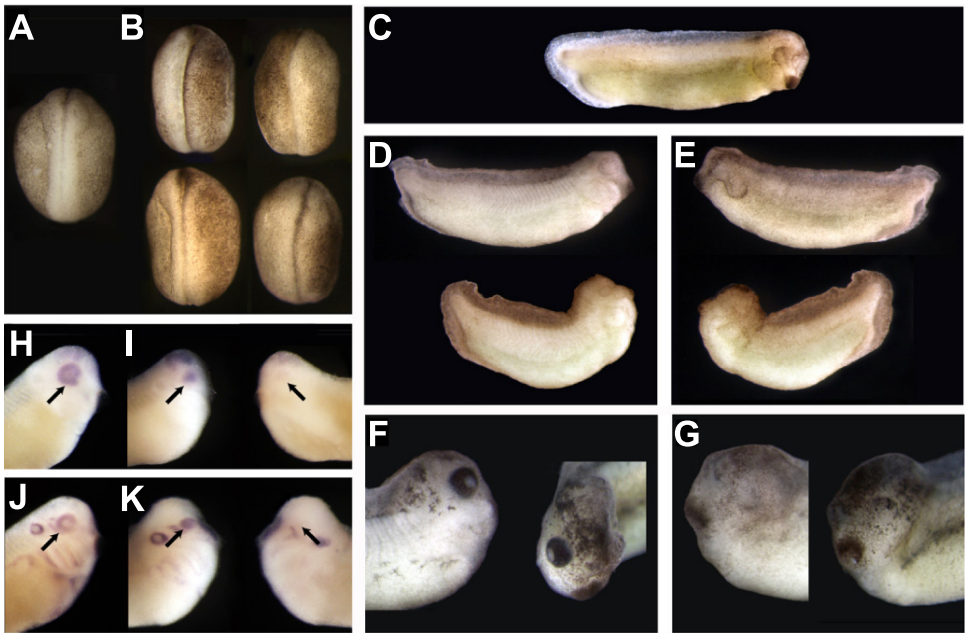

FIGURE 5. **Unilateral injection of XSMOC-1 antisense morpholino (*MO*) produces mild ventralization and anophthalmia on the injected side.** XSMOC-1 MO (6 ng) was injected into a single blastomere at the two-cell stage. At stage 17 (*A* and *B*), mild abnormalities were observed in the developing neural axis of XSMOC-1 MO-injected embryos (*B*). By stage 32 (*C–E*), MO-injected embryos were mildly ventralized (*D* and *E*) compared with controls (*C*). In addition, eyes were absent on the injected side (*E*); this was more apparent by stage 38 (*G*). Eye development appeared normal on the noninjected side (*F*). The XSMOC-1 MO phenotypes shown in *D* and *E* were typical for this stage and were observed in 90% of the embryos in five independent experiments ($n = 164$). *H–K*, whole mount hybridization *in situ* analyses of Otx2 (*H* and *I*) and Tbx2 (*J* and *K*) in stage 32 control (*G* and *J*) and XSMOC-1 MO-injected (*I* and *K*) embryos. The injected sides are displayed on the *right*. The *arrows* indicate the location of the eye fields.

sites (also present in Smad5 and -8) that cannot be phosphorylated by dp-ERK (26) and lacks BMP inhibitory activity. Animal caps from injected embryos were analyzed by RT-PCR for a number of anterior markers (Fig. 9*A*). In the presence of LM-Smad1, XSMOC-1 did not induce the synthesis of the neural markers N-CAM, Otx2, or NRP-1. In contrast, noggin, which acts by direct binding to BMPs, continued to induce these markers in the presence of LM-Smad-1 (Fig. 9*A*). In accordance with LM-Smad-1 inhibiting the activity of XSMOC-1, the epidermal marker, keratin, was expressed in control caps and in the presence of LM-Smad1 or LM-Smad1 plus *X*-SMOC-1 (Fig. 9*A*). Keratin was not detected in the presence of XSMOC-1 alone, noggin, or noggin plus LM-Smad1 (Fig. 9*A*). Further evidence that XSMOC-1 acts through the MAPK signaling pathway was obtained by comparing ERK phosphorylation in control and XSMOC-1-loaded animal caps using an antibody specific for dp-ERK. dp-ERK is the kinase responsible for linker phosphorylation of Smad1, -5, and -8 (27, 28), and XSMOC-1 overexpression was associated with markedly increased levels of dp-ERK (Fig. 9*B*). Conversely, in stage 12.5 XSMOC-1 morpholino-injected embryos, dp-ERK activity was absent in the anterior region of the embryo (Fig. 9*C*).

dp-ERK formation can be inhibited by the chemical inhibitor U0126, which blocks the activity of MAPK/ERK kinase (MEK) (30). Animal caps from XSMOC-1-injected embryos were incubated in the presence or absence of U0126 (50 μM) until control embryos reached stage 17. RT-PCR analysis of anterior neuroectodermal (Otx2 and XAG-1) and panneural (NCAM and NRP-1) markers demonstrated that in the presence of U0126, there was a marked reduction in XSMOC-1 activity (Fig. 9*D*).

DISCUSSION

Previous studies on mammalian SMOC in adult tissues identified two closely related genes, *SMOC-1* and *-2*, which have been characterized as extracellular calcium-binding proteins (4, 5) with angiogenic and growth factor-potentiating activities (6). Unlike mammals, the *Xenopus* genome appears to contain only one *SMOC* gene, the ortholog of mammalian *SMOC-1*. The domain structure of XSMOC-1 and mammalian SMOC1/2 is conserved, and there is a high degree of identity within each of the domains, with the exception of the region exhibiting no homology to other proteins (see Fig. S1). We observed XSMOC-1 to be a zygotic transcript initially expressed at the anterior of the embryo at the end of gastrulation and onset of neurulation (Fig. 1). In neurula embryos, XSMOC-1 was expressed lateral to the developing neural plate (Fig. 1*C*) and at the early tail bud stage was present in the early pronephric anlage (Fig. 1*F*). In addition to the pronephric expression, later tail bud embryos expressed XSMOC-1 in the ventral region of the developing eye (Fig. 1, *H* and *K*), the lateral aspects of the midbrain and hindbrain (Fig. 1, *I*, *J*, and *L*), and trunk neural crest cells passing laterally to the somites (Fig. 1*M*). To examine SMOC function during embryological development, we used various assays in the *Xenopus* model system.

Overexpression of XSMOC-1 in *Xenopus* embryos produced a dorsalized phenotype and pattern of marker induction suggestive of a BMP antagonist (19, 20). Similar to the BMP antagonists noggin and chordin, XSMOC-1 induced anterior (Otx2, Nrp-1, and XAG) but not posterior (Krox 20) neural markers (Fig. 3). Co-expression experiments in *Xenopus* revealed that XSMOC-1 was able to inhibit the activity of BMP2, which signals through Smad1, -5, or -8 (31), but not activin, which signals through Smad2 or -3 (Fig. 8). Inhibition of BMP2 signaling by XSMOC-1 was also demonstrated in mouse 3T3 fibroblasts (Fig. 8*D*). Unlike noggin and chordin, which are first expressed in the Spemann organizer near the onset of gastrulation, XSMOC-1 was not expressed until the end of gastrulation (stage 12.5) and at the pole opposite to the organizer (Fig. 1*B*). This pattern is consistent with a developmental role for XSMOC-1 in processes initiated following the onset of gastrulation. At later stages (20–26), XSMOC-1 expression in the developing pronephros (Fig. 1, *F–J* and *M*) and the ventral region of the developing eye (Fig. 1, *H* and *K*) suggests a possible role in the organogenesis of these structures. Potential targets

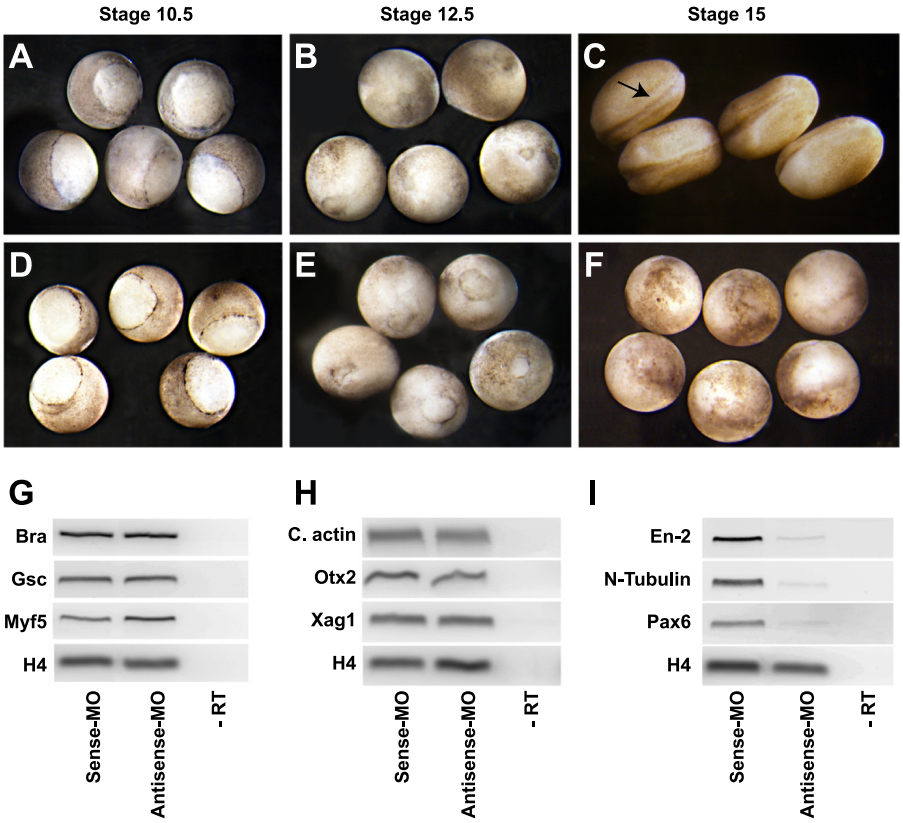

FIGURE 6. **Complete loss of XSMOC-1 function leads to developmental arrest prior to neurulation.** *A–F*, embryos injected bilaterally at the two-cell stage with 6 ng of 5-base mismatch control (*A–C*) or antisense (*D–F*) XSMOC-1 MO. Control MO-injected embryos developed normally (the position of the neural tube is indicated in *C* by an *arrow*), whereas antisense MO-injected embryos appeared normal up to the end of gastrulation (stage 12) but arrested prior to neurulation. The XSMOC-1 MO phenotypes shown in *F* were typical for this stage and were observed in 95% of the embryos in eight independent experiments ($n = 326$). *G–I*, RT-PCR analyses of markers expressed by control and antisense-XSMOC-1 MO-injected embryos at stage 10.5 (*G*), 12 (*H*), and 15 (*I*). Marker expression appeared normal up to stage 12 (*G* and *H*), but markers normally expressed after gastrulation were diminished (*I*). *−RT*, without reverse transcriptase.

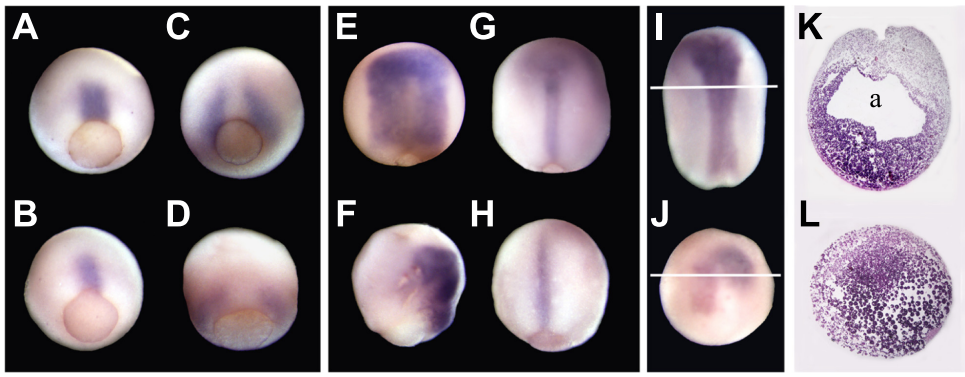

FIGURE 7. Whole mount hybridization *in situ* of control (*A*, *C*, *E*, *G*, and *I*) and antisense XSMOC-1 MO-injected (*B*, *D*, *F*, *H*, and *J*) embryos showing expression of XNot (*A* and *B*) and XMyf5 (*C* and *D*) in stage 11–11.5 embryos, XSox2 (*E* and *F*) and XNot (*G* and *H*) in stage 12.5 embryos, and XSox2 (*I* and *J*) in stage 15 embryos. *K* and *L*, histological sections through *I* and *J* showing absence of archenteron (*a*) and any recognizable dorsal structures in antisense XSMOC-1 MO-injected embryos (modified Von Gieson stain).

for the BMP antagonist activity of XSMOC-1 would be BMP7 in the pronephros (31, 32) and BMP4, BMP7, and GDF6 in the developing eye (33–35).

Of the many BMP antagonists described to date, including noggin, chordin, follistatin, cerberus, dan, and gremlin (for a review, see Ref. 1), most act by direct interaction with BMP ligands to prevent receptor binding or activation. To test whether XSMOC-1 was acting by a similar mechanism, we used a constitutively active type I BMP serine/threonine kinase receptor (caBMPR1B), which activates BMP2/4/7 signaling even in the absence of ligand (25, 36). In the presence of caBMPR1B, noggin did not induce the expression of anterior neural markers in animal cap assays (Fig. 8*E*), consistent with expectations. If XSMOC-1 were acting by a similar mechanism, it would also be expected to be ineffective in the presence of the constitutively active receptor. This was not the case; XSMOC-1 continued to induce expression of anterior neural markers when co-expressed with caBMPR1B (Fig. 8*E*). We conclude, therefore, that the mechanism by which extracellular XSMOC-1 acts as a BMP antagonist appears not to be primarily via direct binding to BMPs but at a point downstream of the receptor.

Activated BMP receptor serine/threonine kinases phosphorylate intracellular Smads (R-Smads) at C-terminal serine residues, resulting in their translocation to the nucleus to form transcriptional complexes (for a review, see Ref. 26). An alternative mechanism for interfering with BMP signaling is via activation of the MAPK pathway upon ligand (*e.g.* epidermal growth factor, fibroblast growth factor, or insulin-like growth factor) binding to tyrosine kinases (27–29). The resulting intracellular phosphorylation of the MAPK, ERK, produces dp-ERK. This, in turn, phosphorylates Smad1, -5, and -8 on serine residues at four conserved P*X*SP sites within the linker region (27, 28). As a consequence, linker-phosphorylated Smad is bound by the ubiquitin ligase Smurf1, resulting in polyubiquitinization and proteasome-dependent degradation in addition to inhibition of Smad nuclear translocation (29). This sequence of events leads to an inhibition of BMP signal transduction. It has been shown that a mutant form of Smad1 (LM-Smad1), which cannot be phosphorylated within the linker region, is unable to inhibit BMP activity (27). When LM-Smad1 was overexpressed in *Xenopus* embryos, XSMOC-1 activity was lost (Fig. 9*A*), indicating that

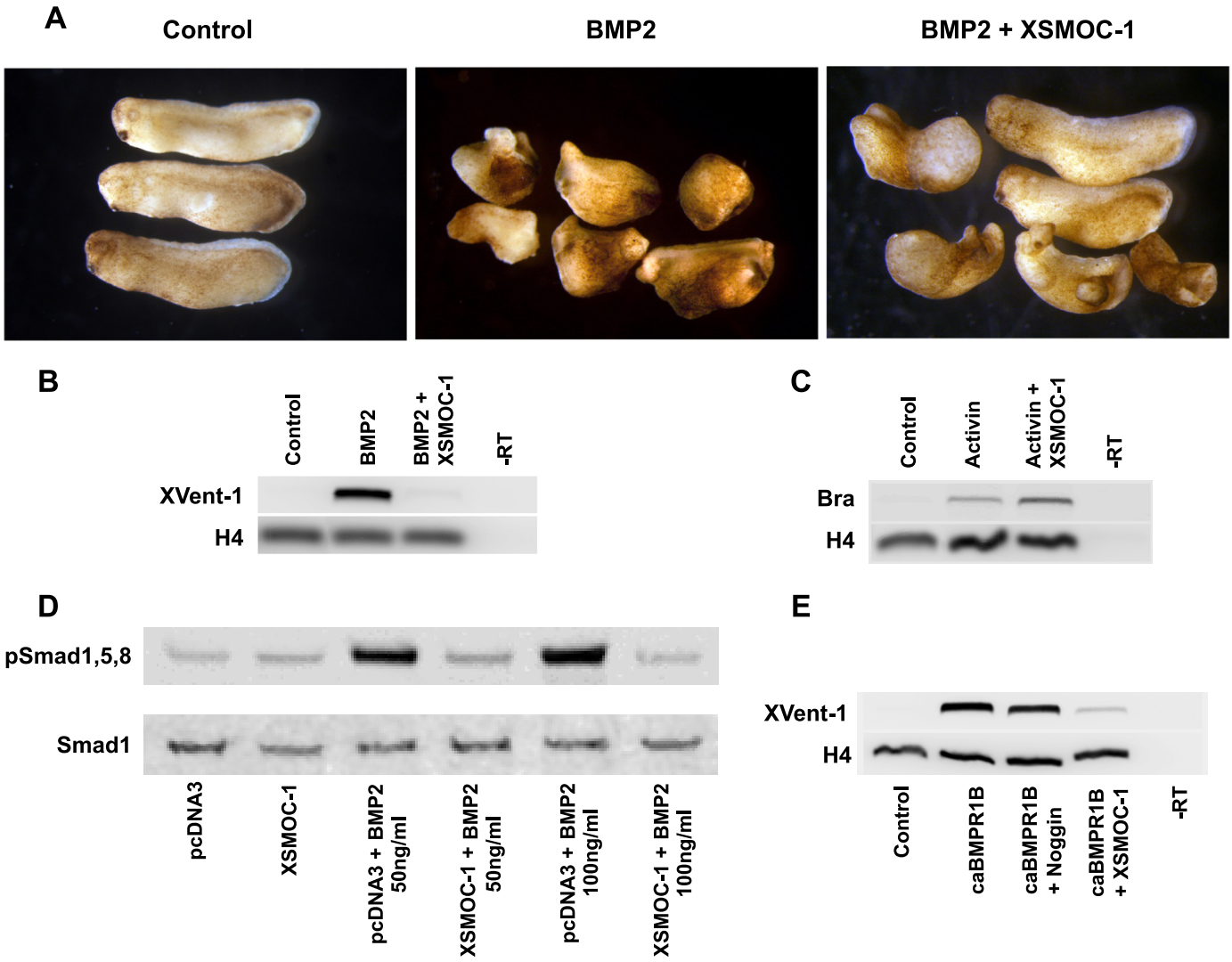

FIGURE 8. **XSMOC-1 inhibits BMP2 activity, but not by direct ligand binding.** *A*, embryos were injected bilaterally at the two-cell stage with 360 pg of GFP (control), 60 pg of BMP2 plus 300 pg of GFP, or 60 pg of BMP2 plus 300 pg of XSMOC-1 mRNAs and incubated until stage 26. In three independent experiments, BMP2-injected embryos were ventralized (82% ≤ dorso-anterior index of 1, $n = 84$), whereas those co-injected with BMP2 and XSMOC-1 showed partial to complete rescue (70% ≥ dorso-anterior index of 3 or greater, $n = 98$). *B* and *C*, RT-PCR analysis of animal cap explants removed from embryos at stage 8 and cultured until sibling embryos reached stage 17. *B*, RT-PCR for the ventral marker XVent-1 was induced in caps overexpressing BMP2 but not in control injected caps or caps co-expressing BMP2 and XSMOC-1. *C*, RT-PCR analysis of animal cap explants removed from embryos injected bilaterally at the two-cell stage with 400 pg of GFP (control), 100 pg of activin plus 300 pg of GFP, or 100 pg of activin plus 300 pg of XSMOC-1 mRNAs incubated until stage 17. Expression of the mesodermal marker Brachyury (*Bra*), induced in caps overexpressing activin, was not inhibited by co-expression of XSMOC-1. *D*, immunoblot analysis of mouse 3T3 fibroblast cell lysates. 3T3 fibroblasts were transfected with or without XSMOC-1 and exposed to BMP2 for 1 h. Phosphorylation of Smad1, -5, and -8 by BMP2 was blocked in cells transfected with XSMOC-1. *E*, RT-PCR analysis of animal cap explants removed from embryos injected bilaterally at the two-cell stage with 450 pg of GFP (control), 150 pg of caBMPR1B plus 300 pg of GFP, or 150 pg of caBMPR1B plus 300 pg of XSMOC-1 mRNAs were incubated until stage 17. The expression of the ventral marker XVent-1, induced by overexpression of constitutively active BMP receptor IB (caBMPR1B), was blocked by co-expression with XSMOC-1 but not by noggin. −*RT*, without reverse transcriptase.

XSMOC-1 elicits its effect on BMP signaling by inducing linker phosphorylation of Smad1, -5, or -8. If this is correct, then one might expect there to be an elevation in dp-ERK levels in response to *X*-SMOC1 overexpression. This was the case; immunoblot analysis of animal cap explants overexpressing XSMOC-1 demonstrated a dramatic increase in the level of dp-ERK (Fig. 9*B*). Further support for XSMOC-1 acting via the MAPK pathway came from studies using the MEK inhibitor U0126 (30). In the presence of U0126, XSMOC-1 activity, as measured by its ability to induce neural markers, was markedly reduced. Exactly how extracellular XSMOC-1 produces an elevation in intracellular dp-ERK will be the emphasis of further study.

The modular structure of XSMOC-1 may provide for its interaction at the cell surface, possibly via some kind of direct or indirect interaction with one or more receptor tyrosine kinase(s). Potential interactions involving the N-terminal SMOC follistatin-like domain are unlikely, since a deletion construct lacking this domain was found to have activity comparable with that of wild type XSMOC-1.[5] Further characterization of the modules required for XSMOC-1 activity is ongoing.

Loss of function experiments using antisense morpholino oligonucleotides indicated that the expression of XSMOC-1 is

[5] J. T. Thomas and M. Moos, unpublished results.

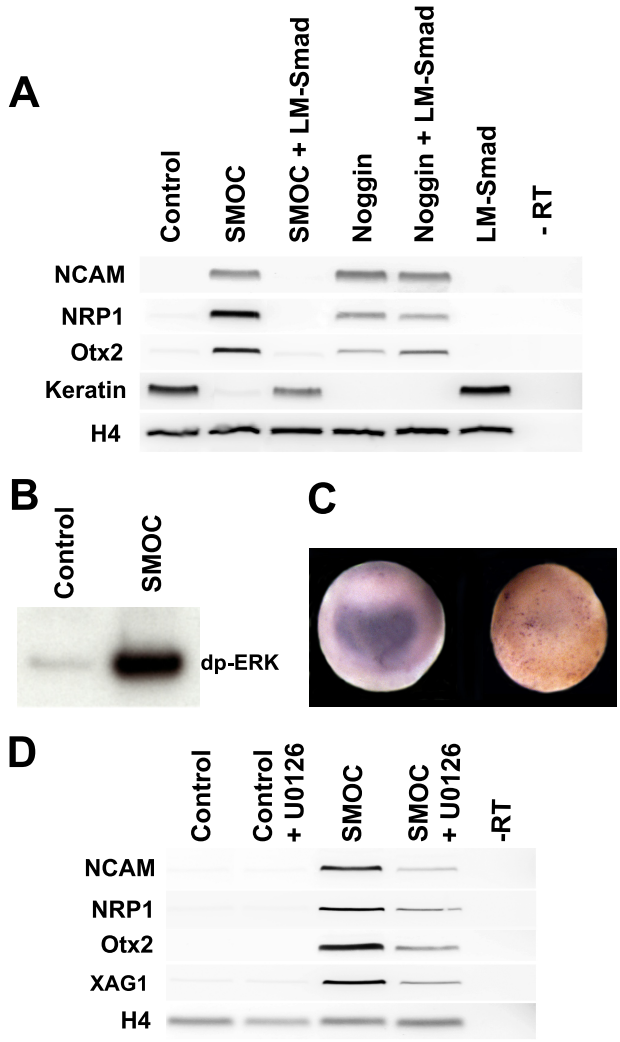

FIGURE 9. **Evidence that XSMOC-1 signals through the MAPK pathway.** *A*, XSMOC-1 activity was blocked by co-expression of LM-Smad1. RT-PCR analysis of animal caps from embryos injected bilaterally at the two-cell stage with 300 pg of XSMOC-1 plus 600 pg of GFP, 300 pg of XSMOC-1 plus 600 pg of LM-Smad1, 6 pg of noggin plus 900 pg of GFP, or 6 pg of noggin plus 600 pg of LM-Smad1 and 300 pg of GFP mRNAs. Induction of the neural markers N-CAM, NRP1, and Otx2 by overexpression of XSMOC-1 was blocked by co-expression of LM-Smad1; expression of the epidermal marker keratin was maintained. Neural marker induction (and suppression of keratin) by overexpression of noggin was not affected by co-expression of LM-Smad1. *B*, immunoblot analysis of animal cap extracts from embryos overexpressing XSMOC-1 revealed elevated levels of dp-ERK. Equivalent amounts of protein (10 mg) were loaded per lane. *C*, anterior views of control (*left*) and XSMOC-1 MO-injected stage 12.5 embryos immunostained for dp-ERK, Note the absence of dp-ERK in the XSMOC-1 MO-injected embryo. *D*, RT-PCR analysis of animal caps from XSMOC-1-injected embryos incubated in the presence or absence of the MEK inhibitor U0126 (50 μM) until control embryos reached stage 17. Anterior neuroectodermal (Otx2 and XAG-1) and panneural (NCAM and NRP-1) markers induced by XSMOC-1 were markedly reduced in the presence of U0126. *−RT*, without reverse transcriptase.

essential for development to proceed through neurulation and subsequent dorsal patterning. In the absence of XSMOC-1, gastrulation and neural induction appeared normal, but embryological development arrested just prior to neurulation (Fig. 6*F*), in a manner suggestive of the phenotype observed following simultaneous knockdown of chordin, follistatin, and noggin (37). However, these antagonists are expressed during gastrulation in or near the Spemann organizer, and thus are probably influencing a set of events distinct in both space and time from those modulated by XSMOC-1.

The severity of the phenotype we observed in bilaterally injected morphant embryos prompted us to consider the possibility that loss of XSMOC-1 function was somehow affecting a vital "housekeeping" function. We believe this to be unlikely. First, XSMOC-1 MO-unilaterally injected embryos showed specific defects in anterior structures (Fig. 5), a result that would not be expected if a gene required by every cell was disrupted. Second, posterior structures were normal on both sides of unilaterally injected embryos. Third, the conjugated cap experiment (Fig. 4, *B* and *C*) demonstrated XSMOC-1 to be non-cell-autonomous, whereas housekeeping proteins are cell-autonomous. These observations are incompatible with a ubiquitous nonspecific housekeeping function for XSMOC-1.

It has been well documented that inhibition of BMP signaling is paramount for neural induction (for a review, see Ref. 1). During gastrulation, the Spemann organizer and closely neighboring tissue secrete a number of proteins that bind BMPs and antagonize BMP signaling in adjacent cells, allowing them to follow their default neural pathway (1, 38–40). Considerable functional redundancy exists between these BMP inhibitors; depletion of any one or even two does not result in loss of the neural plate (37). Simultaneous depletion of three (chordin, noggin, and follistatin) is required before complete failure of dorsal patterning is achieved (37). The apparent absolute requirement for XSMOC-1 for neurulation and subsequent development, suggested by our loss-of-function data (Fig. 6), is thus somewhat surprising. It is unusual that a protein with such an important function during development has no redundancy. Analyses of different genomes reveals that the nonredundancy of SMOC in *Xenopus* may be limited to amphibians, since there are two *SMOC* genes in zebrafish, chickens, mice, and humans.

In normal *Xenopus* embryos, many molecular markers associated with neural induction are present before XSMOC-1 expression can be detected. The expression of these early neural markers during gastrulation was not affected by XSMOC-1 depletion (Figs. 6*G* and 7, *B* and *D*), suggesting that the effect of XSMOC-1 is not on primary neural induction but on subsequent neurulation events needed for specification of the nervous system. In agreement with this hypothesis, the markers N-tubulin (neuronal differentiation), Engrailed (midbrain/hindbrain boundary), and Pax6 (anterior neural tissue), which are expressed postgastrulation, were markedly reduced (Fig. 6*I*). In addition, the neural plate marker Sox2 was expressed aberrantly (Fig. 7, *F* and *J*). The sudden and dramatic developmental arrest immediately following apparently normal gastrulation suggests that XSMOC-1 may have an essential function in one or more of the mechanical events necessary for neurulation. The abnormalities in spatial distribution of Myf5 and Xnot apparent in bilaterally injected stage 12 morphant embryos (Fig. 7, *B* and *D*), indicating disruption of developmental fields secondary to abnormal morphogenetic movements, are consistent with this possibility. Neurulation is defined as a set of morphogenetic or convergent extension movements that result in formation of the neural tube, future brain, and spinal cord (for a review, see Ref. 41). This process requires the coordinated reorganization of cell-cell and cell-matrix interactions. One

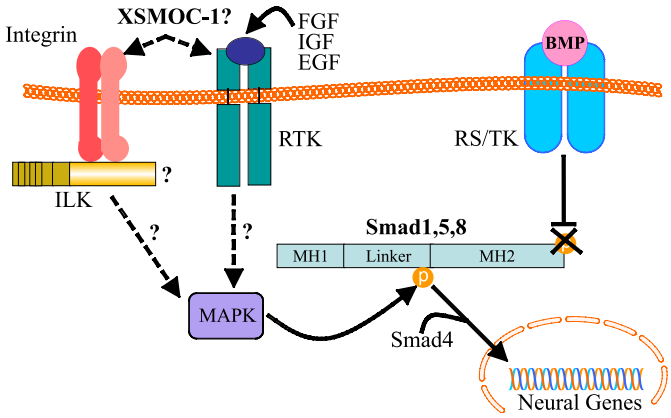

FIGURE 10. **Schematic representation depicting the known and unknown molecular interactions resulting in negative regulation of BMP signaling by XSMOC-1.** The *diagram* shows the BMP receptor serine/threonine kinase (*RS/TK*), fibroblast growth factor (*FGF*), epidermal growth factor (*EGF*), insulin-like growth factor (*IGF*), receptor tyrosine kinase (*RTK*), integrin-linked kinase (*ILK*), and MAPK.

group of molecules involved in these types of interactions is the integrin family of transmembrane proteins. Integrins have a structural role, linking the extracellular matrix to the intracellular actin cytoskeleton, but also activate signaling pathways regulating cell migration, differentiation, growth, and survival (for a review, see Ref. 42). Interestingly, an abrupt arrest in *Xenopus* development at the onset of neurulation, as observed following XSMOC-1 depletion, is also observed in the absence of α6 integrin (43, 44). A possible link between integrins and SMOC comes from studies in the mammalian system, where SMOC-1 is described as a calcium-binding protein often localized to basement membranes (5). Basement membrane matrices interact with cell surfaces via the extracellular domains of integrins (45), and both the BM-40 family member SPARC (46) and mammalian SMOC-2 (11) have been shown to be involved in activation of the cytoplasmic integrin effector, integrin-linked kinase. There is also substantial evidence that integrins are involved in MAPK signaling (42, 47). Consequently, possible interactions between XSMOC-1, integrins, and/or receptor-tyrosine kinases warrant further investigation (Fig. 10).

In summary, we present evidence that the BM-40 family member XSMOC-1 acts as an antagonist of BMPs that signal through Smad1, -5, or -8 by activation of an intracellular MAPK cascade culminating with phosphorylation of the Smad linker region. The BMP antagonist activity of XSMOC-1, coupled with its localization within basement membranes, could allow for discrete localization of BMP inhibitory activity and provide a mechanism for establishing sharp developmental field boundaries. In addition, our loss-of-function data demonstrate that XSMOC-1 is essential to neurulation and subsequent developmental events.

Acknowledgments—We thank Deborah Hursh and Steven Bauer for critical review of the manuscript and Przemko Tylzanowski for sharing unpublished data. We are grateful to Tony Ferrine, Mario Hernandez, and Keith Black for superb care of the Xenopus colony.

REFERENCES

1. Vonica, A., and Brivanlou, A. H. (2006) *Semin. Cell Dev. Biol.* **17,** 117–132
2. Chang, S. C., Hoang, B., Thomas, J. T., Vukicevic, S., Luyten, F. P., Ryba, N. J., Kozak, C. A., Reddi, A. H., and Moos, M., Jr. (1994) *J. Biol. Chem.* **269,** 28227–28234
3. Hoang, B., Moos, M., Jr., Vukicevic, S., and Luyten, F. P. (1996) *J. Biol. Chem.* **271,** 26131–26137
4. Vannahme, C., Gösling, S., Paulsson, M., Maurer, P., and Hartmann, U. (2003) *Biochem. J.* **373,** 805–814
5. Vannahme, C., Smyth, N., Miosge, N., Gösling, S., Frie, C., Paulsson, M., Maurer, P., and Hartmann, U. (2002) *J. Biol. Chem.* **277,** 37977–37986
6. Rocnik, E. F., Liu, P., Sato, K., Walsh, K., and Vaziri, C. (2006) *J. Biol. Chem.* **281,** 22855–22864
7. Raines, E. W., Lane, T. F., Iruela-Arispe, M. L., Ross, R., and Sage, E. H. (1992) *Proc. Natl. Acad. Sci. U.S.A.* **89,** 1281–1285
8. Kupprion, C., Motamed, K., and Sage, E. H. (1998) *J. Biol. Chem.* **273,** 29635–29640
9. Hasselaar, P., and Sage, E. H. (1992) *J. Cell. Biochem.* **49,** 272–283
10. Francki, A., Bradshaw, A. D., Bassuk, J. A., Howe, C. C., Couser, W. G., and Sage, E. H. (1999) *J. Biol. Chem.* **274,** 32145–32152
11. Liu, P., Lu, J., Cardoso, W. V., and Vaziri, C. (2008) *Mol. Biol. Cell* **19,** 248–261
12. Gurdon, J. B. (1967) in *Methods in Developmental Biology* (Wilt, F. H., and Wessels, N. K., eds) pp. 75–84, Crowell, New York
13. Sive, H. L., Grainger, R. M., and Harland, R. M. (2000) *Early Development of Xenopus laevis*, Cold Spring Harbor Laboratory, Cold Spring Harbor, NY
14. Nieuwkoop, P. D., and Faber, J. (1994) *Normal Table of Xenopus laevis* (Daudin) Garland Publishing, Inc., New York
15. Keller, R. (1991) *Methods Cell Biol.* **36,** 61–113
16. Moos, M., Jr., Wang, S., and Krinks, M. (1995) *Development* **121,** 4293–4301
17. Kao, K. R., and Elinson, R. P. (1988) *Dev. Biol.* **127,** 64–77
18. Harland, R. M. (1991) *Methods Cell Biol.* **36,** 685–695
19. Cooke, J. (1979) *J. Embryol. Exp. Morph.* **51,** 165–182
20. Hsu, D. R., Economides, A. N., Wang, X., Eimon, P. M., and Harland, R. M. (1998) *Mol. Cell* **1,** 673–683
21. Smith, W. C., and Harland, R. M. (1992) *Cell* **70,** 829–840
22. Heasman, J. (2002) *Dev. Biol.* **243,** 209–214
23. Clement, J. H., Fettes, P., Knöchel, S., Lef, J., and Knöchel, W. (1995) *Mech. Dev.* **52,** 357–370
24. Lin, J., Patel, S. R., Cheng, X., Cho, E. A., Levitan, I., Ullenbruch, M., Phan, S. H., Park, J. M., and Dressler, G. R. (2005) *Nat. Med.* **11,** 387–393
25. Zou, H., Wieser, R., Massagué, J., and Niswander, L. (1997) *Genes Dev.* **11,** 2191–2203
26. Massagué, J., Seoane, J., and Wotton, D. (2005) *Genes Dev.* **19,** 2783–2810
27. Kretzschmar, M., Doody, J., and Massagué, J. (1997) *Nature* **389,** 618–622
28. Pera, E. M., Ikeda, A., Eivers, E., and De Robertis, E. M. (2003) *Genes Dev.* **17,** 3023–3028
29. Sapkota, G., Alarcón, C., Spagnoli, F. M., Brivanlou, A. H., and Massagué, J. (2007) *Mol. Cell* **25,** 441–454
30. Favata, M. F., Horiuchi, K. Y., Manos, E. J., Daulerio, A. J., Stradley, D. A., Feeser, W. S., Van Dyk, D. E., Pitts, W. J., Earl, R. A., Hobbs, F., Copeland, R. A., Magolda, R. L., Scherle, P. A., and Trzaskos, J. M. (1998) *J. Biol. Chem.* **273,** 18623–18632
31. Hoodless, P. A., Haerry, T., Abdollah, S., Stapleton, M., O'Connor, M. B., Attisano, L., and Wrana, J. L. (1996) *Cell* **85,** 489–500
32. Dudley, A. T., Lyons, K. M., and Robertson, E. J. (1995) *Genes Dev.* **9,** 2795–2807
33. Wang, S., Krinks, M., Kleinwaks, L., and Moos, M., Jr. (1997) *Genes Funct.* **1,** 259–271
34. Chang, C., and Hemmati-Brivanlou, A. (1999) *Development* **126,** 3347–3357
35. Hemmati-Brivanlou, A., and Thomsen, G. H. (1995) *Dev. Genet.* **17,** 78–89
36. Wieser, R., Wrana, J. L., and Massagué, J. (1995) *EMBO J.* **14,** 2199–2208
37. Khokha, M. K., Yeh, J., Grammer, T. C., and Harland, R. M. (2005) *Dev. Cell* **8,** 401–411

38. Harland, R., and Gerhart, J. (1997) *Annu. Rev. Cell Dev. Biol.* **13,** 611–667
39. Hemmati-Brivanlou, A., and Melton, D. (1997) *Cell* **88,** 13–17
40. Weinstein, D. C., and Hemmati-Brivanlou, A. (1999) *Annu. Rev. Cell Dev. Biol.* **15,** 411–433
41. Wallingford, J. B., Fraser, S. E., and Harland, R. M. (2002) *Dev. Cell* **2,** 695–706
42. Yamada, K. M., and Even-Ram, S. (2002) *Nat. Cell Biol.* **4,** E75–76
43. Lallier, T. E., and DeSimone, D. W. (2000) *Dev. Biol.* **225,** 135–150
44. Lallier, T. E., Whittaker, C. A., and DeSimone, D. W. (1996) *Development* **122,** 2539–2554
45. Paulsson, M. (1992) *Crit. Rev. Biochem. Mol. Biol.* **27,** 93–127
46. Barker, T. H., Baneyx, G., Cardó-Vila, M., Workman, G. A., Weaver, M., Menon, P. M., Dedhar, S., Rempel, S. A., Arap, W., Pasqualini, R., Vogel, V., and Sage, E. H. (2005) *J. Biol. Chem.* **280,** 36483–36493
47. Giancotti, F. G., and Tarone, G. (2003) *Annu. Rev. Cell Dev. Biol.* **19,** 173–206
48. Gawantka, V., Delius, H., Hirschfeld, K., Blumenstock, C., and Niehrs, C. (1995) *EMBO J.* **14,** 6268–6279